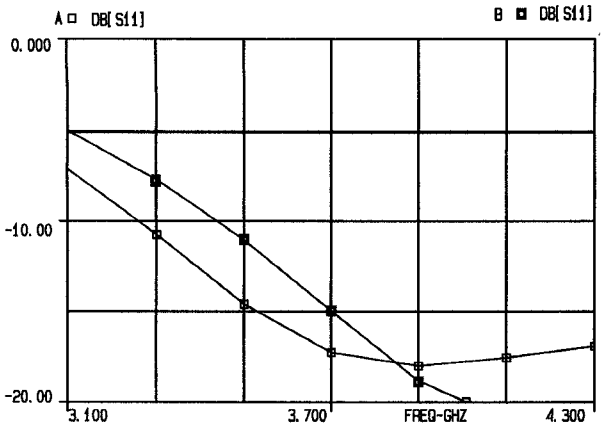

Fig. 6. Input reflection coefficient before (B) and after (A) yield optimization.

to achieve the advantages of physic-based model maintaining the features of lumped-element MESFET model.

The advantages of performing nonlinear yield analysis adopting such a kind of MESFET model demonstrate the importance to devote further efforts in the derivation of new and accurate large-signal model based on lumped elements directly related, by closed expressions, to the MMIC process parameters.

REFERENCES

[1] J. W. Bandler, R. M. Biernacki, Q. Cai, S. H. Chen, S. Ye, and Q. J. Zhang, "Integrated physics-oriented statistical modeling simulation and optimization," *IEEE Trans. Microwave Theory Tech.*, Special Issue on Process-Oriented Microwave CAD and Modeling, vol. 40, pp. 1374–1400, July 1992.

[2] F. Filicori, G. Ghione, and C. U. Naldi, "Physics-based electron devices modeling and computer-aided MMIC design," *IEEE Trans. Microwave Theory Tech.*, Special Issue on Process-Oriented Microwave CAD and Modeling, vol. 40, pp. 1333–1352, July 1992.

[3] D. E. Stoneking, G. L. Bilbro, P. A. Gilmore, R. J. Trew, and C. T. Kelley, "Yield optimization using a GaAs process simulator coupled to a physical devices model," *IEEE Trans. Microwave Theory Tech.*, Special Issue on Process-Oriented Microwave CAD and Modeling, vol. 40, pp. 1353–1363, July 1992.

[4] E. M. Bastida, G. Donzelli, and M. Pagani, "Efficient development of mass producible MMIC circuits," *IEEE Trans. Microwave Theory Tech.*, Special Issue on Process-Oriented Microwave CAD and Modeling, vol. 40, pp. 1364–1373, July 1992.

[5] J. C. Sarker and J. E. Purviance, "Yield sensitivity of HEMT circuits to process parameter variations," *IEEE Trans. Microwave Theory Tech.*, Special Issue on Process-Oriented Microwave CAD and Modeling, vol. 40, pp. 1572–1576, July 1992.

[6] D. L. Allen, J. Beall, and M. King, "Small-signal RF yield analysis of MMIC circuit based on physical device parameters," in *Proc. IEEE MTT-S Dig.*, 1992, pp. 1473–1476.

[7] S. D'Agostino, G. D'Inzeo, P. Marietti, L. Tudini, and A. Betti-Berutto, "Analytic physics-based expressions for the empirical parameters of the Statz-Pucel MESFET model," *IEEE Trans. Microwave Theory Tech.*, Special Issue on Process-Oriented Microwave CAD and Modeling, vol. 40, pp. 1576–1581, July 1992.

[8] S. D'Agostino and A. Betti-Berutto, "Physics-based expression for the nonlinear capacitances of the MESFET equivalent circuit," *IEEE Trans. Microwave Theory Tech.*, vol. 42, pp. 403–406, Mar., 1994.

[9] H. Statz, R. A. Pucel, and H. A. Haus, "GaAs FET device and circuit simulation in spice," *IEEE Trans. Electron Devices*, vol. ED-34, no. 2, pp. 160–169, Feb. 1987.

[10] Touchstone & Libra, User's Guide, *EEsof*, 1993.

[11] M. S. Shur, "Analytical model of GaAs FET's," *IEEE Trans. Electron Devices*, vol. 32, pp. 70–72, Jan. 1985.

[12] R. Goyal, *Monolithic Microwave Integrate Circuit Technology and Design*. Norwood, MA: Artech House, 1989.

28 GHz Omni-Directional Quasi-Optical Transmitter Array

Mark J. Vaughan and Richard C. Compton

***Abstract*—Omni-directional base stations are needed in many emerging wireless communication systems. This paper presents the first adaptation of a quasi-optical oscillator array for this purpose. A 28 GHz active oscillator element containing a modified Vivaldi endfire antenna is utilized as the unit cell. Twelve of these are incorporated into the circular array, which is powered from a single dc power supply. The array has a high combining efficiency and remains frequency-locked over a span of 600 MHz.**

I. INTRODUCTION

Because of the low millimeter-wave output power available from solid-state devices, it will be necessary for many applications (aside from those where vacuum tubes are acceptable) to use a plurality of devices to generate adequate amounts of power. Quasi-optical arrays use free-space combination to efficiently sum the outputs of multiple devices [1].

To date, quasi-optical research has focused on planar arrays to replace traveling-wave tubes for point-to-point and radar applications. The printed-circuit type antennas integrated into these arrays nearly all operate broadside. These include the microstrip patches [2], [3], the grid antennas [4], slot antennas [5], [6], waveguide probes [7], and dipoles [8]. The only exceptions are antennas used with dielectric waveguide resonators [9] and the tapered slot antennas (TSA), which can be found in a variety of endfire applications [10]–[13]. However, these, like the broadside antennas, have strictly been used in active arrays for directing the output power into a single direction.

These systems are not well suited for local multipoint distribution services (LMDS) where a base station must communicate with multiple subscribers in a cellular configuration. For LMDS an omni-directional transmitter is needed, and the tapered slot antennas are ideal for this purpose. They can be arranged on a single circular planar substrate to radiate azimuthally in all directions [14]. Further, since the active circuits are all located in the center of such an array, they can be monolithically fabricated separately from the antennas. This eliminates the excessive costs of fabricating the relatively large antennas on expensive GaAs substrates. GaAs is also an undesirable antenna substrate because of its high dielectric-constant. The circular nature of the array means that the coupling lines between the elements in an oscillator array form a closed loop, which has been shown in standard rectangular arrays to have benefit in reducing the number of

Manuscript received January 1995; revised June 1995. This work was supported by the Army Research Office. M. Vaughan was supported in part by a National Science Foundation Graduate Research Fellowship and by a JSEP Graduate Fellowship.

The authors are with the School of Electrical Engineering, Cornell University, Ithaca, NY 14853 USA.

IEEE Log Number 9414245.

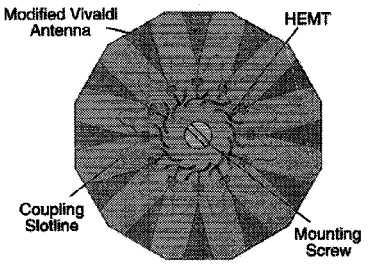

Fig. 1. Twelve element omni-directional array. The array's total width is 4.7 cm. Lighter shaded areas represent metal.

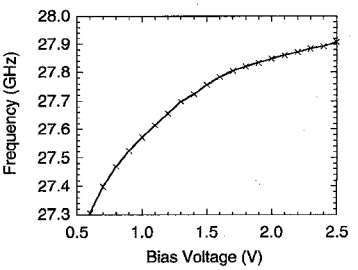

Fig. 2. Variation of frequency with change in dc bias voltage for the array. The array operates over a 600 MHz span.

unwanted modes [15]. Finally, for additional power combining, the arrays can be stacked vertically.

This paper presents the design and measured characteristics of a 12-element, omni-directional 28 GHz oscillator array which, although for development purposes was constructed using hybrid techniques, could easily be fabricated monolithically.

II. Design

The array is designed using a technique first proposed by York [2]. This technique allows the individual elements to be designed and optimized prior to full array construction. For this array, a 28 GHz CPW/slotline oscillator based on a pseudomorphic HEMT and incorporating an endfire antenna is used [16].

The planar antenna in this circuit is a customized version of a Vivaldi TSA, modified to take up less space. This is an important feature, because in the design of this circular array, the radius should generally be made as small as possible to minimize the amount of destructive interference in the array radiation pattern. In other words, the antennas should be close together to create a uniform pattern as a function of azimuth, and reducing the array radius primarily requires reducing the antenna length.

The 12-element array is diagrammed in Fig. 1. In the center of the array is a screw for mounting the array to a support post. The dc ground is also applied through this post. Positive dc bias wires for each oscillator are attached to the edges of the substrate midway between each antenna.

To obtain a reasonably uniform radiation pattern, the oscillators must all operate with similar phases. This requires that the coupling lines have the correct length (an odd multiple of a half-wavelength in this case) and that the oscillators have operating frequencies close to each other. A rough indication of the necessary frequency restrictions can be obtained from the formula

$$\Delta f \sim \Delta f_m \sin \Delta\phi$$

where Δf is the deviation of the oscillator's free-running frequency from the array's design frequency, $\Delta\phi$ is the desired maximum phase deviation, and Δf_m is the locking range of the oscillators (the maximum difference in frequency two oscillators can have and still lock), which in this case is approximately 500 MHz.

For this array it was decided that restricting $\Delta\phi$ to roughly 10° would be adequate for testing the array's characteristics, so the free-running frequencies were mechanically tuned to be within a 100 MHz range, as per the above formula. The oscillators' frequencies were increased by placing bond wires on the source CPW lines between the center conductor and the ground plane, effectively reducing the length of this short-circuited line. Once all were operating within the range 27.96–28.06 GHz, the dc bias wires were connected together.

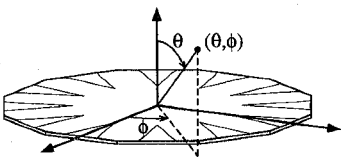

Fig. 3. Definition of elevation (θ) and azimuth (ϕ) coordinates in relation to the array substrate.

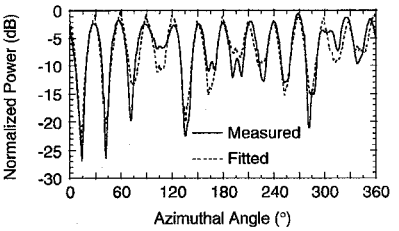

Fig. 4. Radiation pattern for the array measured and computed in the plane of the antennas ($\theta = 90°$) as a function of azimuthal angle, ϕ. The fitted pattern is computed using the single-element E-plane data [16], with oscillator phases fitted to match the measurement. The oscillators are located at 0°, 30°, etc.

III. Measurements

With the 12 oscillators all powered from a single dc power source and locked in frequency, measurements were made of the array's operating characteristics. The oscillators remain locked over the entire range of bias voltage (0.6–2.5 V). Fig. 2 shows a plot of the variation of frequency as a function of bias voltage. As expected, the curve has the same shape as that for the single element [16]. The 3 dB bandwidth for the array, as for the single oscillator, is about 100 MHz, but the maximum dc-rf efficiency occurs at a bias level of about 1.4 V, which is a half volt below the maximum efficiency bias point of the single oscillators.

Antenna pattern measurements were made as functions of elevation and azimuth (see Fig. 3 for angle definitions), with the array biased at 2.0 V, drawing 622 mA and operating at 27.9 GHz. The radiation pattern in the plane of the array (E-plane) is plotted versus azimuthal angle in Fig. 4. Although the E-plane HPBW of the individual elements is 30°, the power between the directions in which the antennas are pointing drops to as much as 25 dB below the peaks due to interference. This is a result of the relatively large spacing between the antennas ($1.1\lambda_0$ between aperture centers at the array perimeter).

The "fitted" curve of Fig. 4 is generated using E-plane data measured for the single element. Each element in the array is modeled as a point source located a fixed distance from the center, operating with the same amplitude and frequency as its neighbors, but not the same phase. This effective radius, the eleven phase parameters, and two offset parameters were fitted so that the resulting computed pattern closely matches the measured data—a nonlinear least-squares

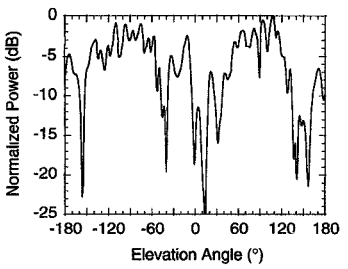

Fig. 5. Array radiation pattern measurement made as function of elevation angle, θ, with $\phi = 0°$.

algorithm based on the Levenberg–Marquardt method [17] was used for the fitting. The results show that the majority of the oscillators are operating within 10° of their two nearest neighbors, and the two largest phase differences are roughly 20° and 30°. These larger values are believed to be a result of frequency detuning of a few oscillators, due to their hybrid construction, during handling of the array. The effective radius (the location of the phase centers) is found to be 2.8 mm less than the physical radius, which is quite reasonable considering that the antenna slot width reaches a half-wavelength 2.5 mm from the edge of the substrate.

The co-pol and cross-pol patterns were measured in twenty-four different planes (azimuthal angle stepped by 7.5°, a quarter-of the angular distance between antennas) with the elevation angle swept from -180 to $+180°$. One of the cuts which includes the directions pointed by two antennas is shown in Fig. 5.

Interpolating the data between the twenty-four cuts based on the E-plane pattern, the total co-polarized radiated power is computed approximately to be 144 mW, which means the combining efficiency is about 87%. (The total radiated power in the co-pol from a single element is about 14 mW.) This corresponds to an EIRP of 0.28 W at a dc-rf efficiency of 11.6%. The total power measured in the cross-pol is 130 mW. Note, however, that this array cross-pol measurement includes contributions from the copolarized radiation of the individual elements.

IV. Future Work

Before this array can be used in a practical system the radiation patterns must be improved. The vertical beam width needs to be reduced to about 10°. This may be possible just by placing flat reflectors above and below the array. Alternatively, multiple arrays could be stacked to narrow the array pattern beamwidth while increasing power output. Further, by stacking the arrays offset 15° in azimuthal angle, simulations predict the ripple in the E-plane pattern can be reduced to 2 dB.

Future work will also make use of higher power devices and demonstrate the application of such an array in a communications system.

V. Summary

The 28 GHz endfire oscillator element of [16] is well suited for use in an omni-directional array. When implemented in a 12–element quasi-optical transmitter, the oscillators are arranged in a circle, making the coupling lines a closed loop. The array is operated from a single dc power source, and the elements remain locked over the entire dc operating range, tuning from 27.3–27.9 GHz. With a moderate bias voltage applied, the array radiates a total co-pol power of 144 mW, which corresponds to an 87% power combining efficiency.

Acknowledgment

The authors would like to thank R. Martinez of IBM and S. Weinreb of Martin Marietta for invaluable discussions. The HEMT's used in the array were donated by P. Smith of GE/Martin Marietta.

References

[1] J. W. Mink, "Quasi-optical power combining of solid-state millimeter-wave sources," *IEEE Trans. Microwave Theory Tech.*, vol. 34, no. 2, pp. 273–279, Feb. 1986.

[2] R. A. York and R. C. Compton, "Quasi-optical power combining using mutually synchronized oscillator arrays," *IEEE Trans. Microwave Theory Tech.*, vol. 39, no. 6, pp. 1000–1009, June 1991.

[3] A. Balasubramaniyan and A. Mortazawi, "Two-dimensional MESFET-based spatial power combiners," *IEEE Microwave Guided Wave Lett.*, vol. 3, no. 10, pp. 366–368, Oct. 1993.

[4] Z. B. Popović, R. M. Weikle II, M. Kim, and D. B. Rutledge, "A 100-MESFET planar grid oscillator," *IEEE Trans. Microwave Theory Tech.*, vol. 39, no. 2, pp. 193–200, Feb. 1991.

[5] M. J. Vaughan and R. C. Compton, "Resonant-tee CPW oscillator and the application of the design to a monolithic array of MESFET's," *Electronics Lett.*, vol. 29, no. 16, pp. 1477–1479, Aug. 5, 1993.

[6] S. Kawasaki and T. Itoh, "Quasi-optical planar arrays with FET's and slots," *IEEE Trans. Microwave Theory Tech.*, vol. 41, no. 10, pp. 1838–1844, Oct. 1993.

[7] N. J. Kolias and R. C. Compton, "A microstrip-based unit cell for quasi-optical amplifier arrays," *IEEE Microwave Guided Wave Lett.*, vol. 3, no. 9, pp. 330–332, Sept. 1993.

[8] G. M. Rebeiz, D. K. Kasilingam, Y. Guo, P. A. Stimson, and D. B. Rutledge, "Monolithic millimeter-wave two-dimensional horn imaging arrays," *IEEE Trans. Antennas Propagat.*, vol. 38, no. 9, pp. 1473–1482, Sept. 1990.

[9] A. Schuneman, S. Zeisberg, P. L. Heron, G. P. Monahan, M. B. Steer, J. W. Mink, and F. W. Schwering, "A prototype quasi-optical slab resonator for low cost millimeter-wave power combining," in *Proc. Workshop on Millimeter-Wave Power Generation and Beam Control*, Redstone Arsenal, AL, Sept. 1993, pp. 235–243.

[10] D. Rascoe, R. Crist, A. L. Riley, T. Cooley, L. Duffy, D. Antsos, V. Lubecke, W. Chew, K. S. Yngvesson, and D. H. Schaubert, "Ka-band MMIC beam steered planar array feed," in *IEEE MTT-S Int. Microwave Symp. Dig.*, Dallas, TX, May 1990, pp. 809–812.

[11] R. N. Simons and R. Q. Lee, "Space power amplification with active linearly tapered slot antenna array," in *IEEE MTT-S Int. Microwave Symp. Dig.*, Atlanta, GA, June 1993, pp. 623–626.

[12] J. A. Navarro, Y. H. Shu, and K. Chang, "Broadband electronically tunable planar active radiating elements and spatial power combiners using notch antennas," *IEEE Trans. Microwave Theory Tech.*, vol. 40, no. 2, pp. 323–328, Feb. 1992.

[13] P. A. Acharya, H. Ekström, S. S. Gearhart, S. Jacobsson, J. F. Johansson, E. L. Kollberg, and G. M. Rebeiz, "Tapered slotline antennas at 802 GHz," *IEEE Trans. Microwave Theory Tech.*, vol. 41, no. 10, pp. 1715–1719, Oct. 1993.

[14] R. N. Simons, E. S. Kelly, R. Q. Lee, and S. R. Taub, "Radial microstrip slotline feed network for circular mobile communications array," in *1994 IEEE AP-S Int. Symp. Dig.*, Seattle, WA, June 1994, pp. 1024–1027.

[15] J. Lin and T. Itoh, "Two-dimensional quasi-optical power-combining arrays using strongly coupled oscillators," *IEEE Trans. Microwave Theory Tech.*, vol. 42, no. 4, pp. 734–741, Apr. 1994.

[16] M. J. Vaughan and R. C. Compton, "28 GHz oscillator for endfire quasi-optical power-combining arrays," to be published in *Electronics Lett*, submitted.

[17] W. H. Press, B. P. Flannery, S. A. Teukolsky, and W. T. Vetterling, *Numerical Recipes*. New York: Cambridge Univ. Press, 1986.